DOI 10.1007/s11595-012-0443-1

Microstructure and Wear Resistance of in situ NbC Particles Reinforced Ni-based Alloy Composite Coating by Laser Cladding

DONG Gang[1,2,3], YAN Biao[1*], DENG Qilin[2], YU Ting[2]

(1. School of Materials Science and Engineering, Tongji University, Shanghai 200092, China; 2. School of Mechanical and Power Engineering, Shanghai Jiaotong University, Shanghai 200030, China; 3. School of Medical Technology and Engineering, Henan University of Science and Technology, Luoyang 471003, China)

Abstract: The in situ synthesized NbC particles reinforced Ni-based alloy composite coating was produced by laser cladding a precursor mixture of Ni-based alloy powder, graphite and niobium powders on a steel substrate. The microstructure, phase composition and wear property of the composite coating were investigated by means of scanning electron microscopy (SEM), X-ray diffraction (XRD) and dry sliding wear test. The experiment results show that the composite coating is homogeneous and free from cracks, and about 0.8 mm thick. The microstructure of the composite coating is mainly composed of NbC particles, CrB type chromium borides, γ-Ni primary dendrites, and interdendritic eutectics. CrB phases often nucleate and grow on the surface of NbC particles or in their close vicinity. NbC particles are formed via in situ reaction between niobium and graphite in the molten pool during the laser cladding process and they are commonly precipitated in three kinds of morphologies, such as quadrangle, cluster, and flower-like shape. Compared with the pure Ni-based alloy coating, the microhardness of the composite coating is increased about 38%, giving a high average hardness of HV0.21000, and the wear rate of the composite coating is decreased by about 32%, respectively. These are attributed to the presence of in situ synthesized NbC particles and their well distribution in the coating.

Key words: in situ synthesis; laser cladding; Ni-based alloy; NbC; wear

1 Introduction

In the past two decades, with development of metal matrix composites (MMCs), Laser cladding of ceramics particulate reinforced composite coatings on various traditional substrates becomes an interesting project. Particularly, various carbides of refractory metals reinforced metal matrix composite coatings have been manufactured to improve wear and corrosion resistance of components[1-6]. The reinforcing phases can be obtained by direct addition of ceramic particles in the clad materials (the method of external addition) and also by in situ formation reactions during laser cladding (the method of in situ synthesis). In this method, the reinforcements are synthesized in a metal matrix by chemical reactions between elements or between element and compound during fabrication process[7]. Compared to the reinforcements made by direct addition, the in situ synthesized reinforcements are much more compatible with the matrix, and the interfaces are much cleaner. Moreover, the in situ synthesized reinforcements are thermodynamically stable and their distribution in the matrix is more uniform, yielding better mechanical properties[8-10].

To date, the in situ synthesized carbides of refractory metals reinforced Ni-based alloy composite coatings by laser cladding on various traditional substrates have been reported by many researches. Among these researches, in situ synthesized WC and TiC hold a leading position within composite coatings because of their metallic character and their high wear resistance due to high hardness[11-14]. However, WC is a line compound, and is apt to dissolve owing to its low free formation enthalpy of 38.5 kJ/mol in the molten pool generated by following up laser beam scanning. The dissolved WC reprecipitates to give either WC with a high carbon level, or W_2C or a brittle η phase, such as M_6C or $M_{12}C$, when the carbon concentration is low. Although TiC has a wide solubility range and

(Received: June 19, 2011; Accepted: Sep. 20, 2011)

DONG Gang (董刚): Ph D Candidate; E-mail: donggang_7766@163.com

*Corresponding author: YAN Biao (严彪): Prof.; Ph D; E-mail: yanbiao@vip.sina.com

Funded by the National Natural Science Foundation of China (No. 50675136 and No. 50375096)

is much more stable than WC because of its free formation enthalpy of 184 kJ/mol, TiC particles will float upward in the molten pool because the density of it is about 4.25 g /cm^3 and lighter than Ni-based alloy, which induce that the volume fraction of TiC particles and the microhardness gradually decreased from the top to the bottom of the coating layer. Among carbides of refractory metals, niobium carbide (NbC) is one of the most important compounds, based on its promising properties, such as high melting point (3600 ℃), high microhardness (2400 kg/mm^2)[15], excellent chemical stability, good wear resistance, and high free formation enthalpy (140.7 kJ/mol), which is higher than the WC (38.5 kJ/mol). Also, the density of NbC is about 7.79 g/cm^3[16] and is heavier significantly than the TiC (4.25 g/cm^3) nearing the density of Ni-based alloy (about 7.94 g/cm^3). Therefore, niobium carbide as the reinforcing phase of the laser cladding Ni-based alloy composite coating may be more attractive than the WC and TiC particles. Unfortunately, to our knowledge, little literature is available on the in situ synthesis of NbC reinforced Ni-based alloy composite coatings by laser cladding of (Nb + C)/Ni-based alloy powder mixture.

The objective of the present work was to produce an in situ synthesized NbC reinforced Ni-base alloy composite coating on AISI 1045 steel substrate by laser cladding (Nb + C)/Ni-based alloy powder mixture. In the present study, the microstructure of the composite coating, the distribution and the morphology of NbC phase in the coatings were reported. The microhardness and the wear resistance of the composite coating were also investigated and compared with those of the pure Ni-based alloy coating.

2 Experimental

Cylindrical specimens of AISI 1045 steel with dimensions of 50 mm × 10 mm were used as the substrates. The chemical composition of the steel was 0.42-0.50 C, 0.50-0.80 Mn, 0.17-0.37 Si, Cr≤0.25, Ni≤0.30, Cu≤0.25 and Fe in balance (all wt%). The surfaces of the samples were degreased, polished with sandpaper, dried and finally rinsed by acetone.

The powder mixture was prepared from pure niobium (99.0wt%), graphite (99.0wt%) and self-fluxing Ni-Cr-B-Si-C powders in fixed ratio. The niobium-graphite powder was 15wt%. The niobium to carbon powder ratio corresponded to that of stoichiometric NbC. The composition of Ni-based alloy powder is listed in Table 1. The average particle sizes of Ni-based alloy, pure niobium and graphite powders were less than 20, 15 and 10 μm, respectively. The powder was preplaced on the surface of substrates using an organic binder, to form a layer of 1.2 mm thickness.

Table 1 Chemical composition of nickel-based alloy powder

Elements	C	Si	B	Cr	Fe	Ni
wt%	0.8	3.5	4.5	15.5	15	Bal.

A 3 kW continuous wave CO_2 laser was used for to produce the coating. The parameters varied were the laser power, beam size, and beam scanning speed. The processing parameters were established after a few trial runs. The criteria for determining the optimum quality of the coatings were based on a compromise of highest hardness, best homogeneity, and lowest occurrence of cracks. On the basis of these criteria, the best processing conditions were determined to be as follows: traverse speed for 10 mm/s, beam diameter for 3 mm, and laser power for 2.5 kW. An overlap of 50% between successive tracks was selected in order to obtain a large area coating on the substrate. An argon atmosphere was used to protect the molten pool from the surrounding air.

After laser cladding, the transverse cross sections of the coating were cut, mounted, polished using standard mechanical polishing procedures and etched using the Aqua regia for morphology examination. The microstructure and composition analysis of the composite coating were examined using scanning electron microscope (SEM) equipped with a energy dispersive spectrometry (EDS). The phases of the composite coating were analyzed by X-ray diffraction (XRD) with a Rigaku D-MAX diffractometer (Cu Kα). The working voltage and current were 40 kV and 100 mA, respectively. The step speed was 2 °/min.

Microhardness profile along the depth direction in the transverse cross section of the coating was measured using DHV-1000 digital micohardness tester with a load of 200 g and a loading time of 15 s.

The dry sliding wear tests were carried out on a MM 200 block-on-ring friction and wear tester at room temperature. The test specimens were machined to block with size of 30mm × 7mm × 6 mm. Before the wear testing, the surfaces of specimens were ground with silicon carbide paper. The specimens were then ultrasonically cleaned in alcohol and acetone until the surfaces were spotless. The ring (40 mm in diameter × 10 mm in width) of the wear couple is made of GCr15 steel with a hardness of 60 HRC, rotated at a constant

speed of 200 r/min. The wear conditions were a normal load of 300 N, a sliding speed of 0.84 m/s and a sliding distance of 1250 m.

The average width of the wear track was measured using a vernier caliper, and the wear volume was calculated using the following formula[17]:

$$V = w\left\{\frac{\pi}{180}r^2\sin^{-1}\left(\frac{b}{2r}\right) - \frac{b}{2}\sqrt{\left(r^2 - \frac{b^2}{4}\right)}\right\} \quad (1)$$

where, w is the width of the specimens (mm), b the width of the wear track (mm) and r the out radius of wear ring (mm). The wear volume loss was calculated after a certain time interval.

The worn surfaces were observed by SEM.

3 Results and discussion

3.1 XRD phase analysis

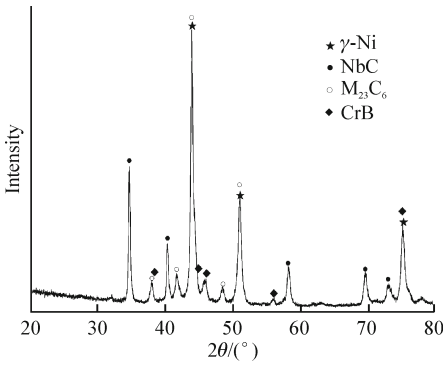

Fig.1 XRD pattern of the composite coating

Fig.1 shows the XRD pattern of the composite coating. It is difficult to identify the reflection in XRD patterns of the coating except for the γ-Ni and NbC phase. One reason is that the interplanar distances corresponding to diffraction peaks of possible phases of the coating are close to each other. Another important reason may be that non-equilibrium solidification involved in the laser cladding results in an extension of solubility and distortion of the lattice, and the formation of metastable phases. However, according to the indexed results of the diffraction peaks in terms of JCPDS cards, it can be found that the composite coating is mainly composed of γ-Ni, NbC, CrB and a little of $M_{23}C_6$. Fig.1 shows that the NbC diffraction peaks are relatively strong, indicating that NbC particles can be formed in situ during laser cladding since the feeding material is the blend of pure Nb, C elements and Ni-based alloy.

3.2 Microstructure and constituents of the composite coating

Fig.2 shows the representative SEM images from transverse section of the composite coating. It can be found that the coating is about 0.8 mm thick and free from cracks. However, very few micro pores could be found within the coating, due to the encapsulated bubbles generated during the laser cladding process, as shown in Fig.2a. It can be found that the white particles are uniformly distributed in the matrix and the dark whisker phases often nucleate and grow on the surface of white particles or in their close vicinity, as shown in Fig. 2b. It can be also seen that there exists a metallurgical bond band with about 2 μm thickness between the coating and the substrate, as shown in Fig.2c. Which come from the planar growth at the bottom of the molten pool. This situation is formed because the substrate at the interface acts as a heat sink, where the temperature gradient (G) is fairly high, but the solidification velocity (V) is very slow. With a sufficiently high G/V ratio, planar crystallization is obtained[18, 19]. Immediately above this, a zone with eutectic morphology can be observed, which consists only of oriented dendrites growing perpendicularly to the interface and interdendritic eutectics. The width of eutectic zone at the bottom of coating is about 25 μm. The other region throughout the coating shows a homogeneous fine microstructure containing a

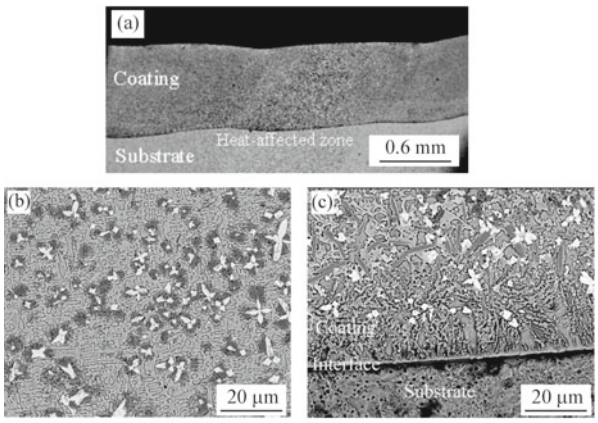

Fig.2 SEM images of the transverse section of (a) whole coating,(b) coating upper and(c) coating/substrate interface

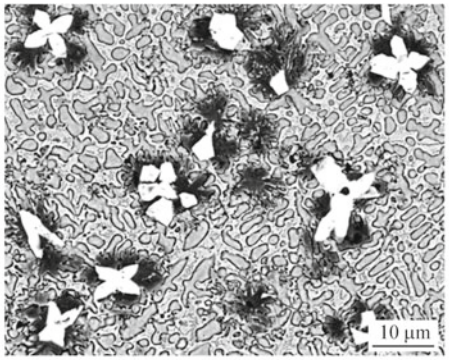

Fig.3 Typical morphologies of NbC particles

large amount of white particles and dark whisker phases. Moreover, the white particles show several morphologies such as approximate quadrangle with size range from 2-5 μm, cluster and flower-like with a width of 5-8 μm and a length of 10-25 μm, respectively, as shown in Fig.3. The amount of cluster and flower-like shape white particles is smaller, and is only present in some local regions.

It is well known that laser cladding is a transient process. The primary precipitated NbC particles may be relatively small due to the high rate of heating and cooling. However, for the multilayer overlapping coating (layer-to-layer), the heat input increases but the solidification rate decreases compare with the single track clad layer owing to the laser beam repetition scanning on the overlapping zone, and there is enough time for a reaction between Nb and C. The growth of NbC carbide crystals is dependent on the continuous and sufficient melt of the constituent atoms of the carbide through the liquid phase. The overlapping process supplies a preferable composition condition and longer duration time for the WC growth. Therefore, there are also a few coarse NbC particles in the clad coating. During laser processing, convection and flow will inevitably exist, so the particles will collide and assemble in the molten pool; some of these are engulfed by advancing solid–liquid interface, resulting in clusters.

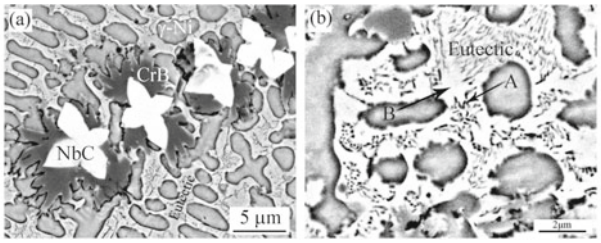

Fig.4 Microstructural details at the upper section of coating: (a) diverse phases existing; (b) magnification showing interdendritic eutectic morphology

Observation of the upper section of coating at higher magnifications (Fig.4a) shows that the microstructure of composite coating consists of fine dendrites, interdendritic eutectics, dark whisker phases and white particles. The results of composition analysis for the various structural constituents in the composite coating are listed in Table 2. According to the results of XRD analysis for the composite coating and with reference to the results of SEM EDS analysis, the phase constitution in the composite coating can be determined. The white phases containing an overwhelmingly high concentration of Nb are mainly composed of Nb and C, in terms of the obtained analysis results, which can be identified as NbC-type carbides. They are primary reinforcements of the composite coating. The dark whisker phases contain an overwhelmingly high concentration of Cr, a smaller amount of Ni, Fe and Nb, a trace of Si, and also contain boron and carbon. The dark whisker phases, therefore, could be determined as primary carbon bearing chromium boride. Considering the XRD result, the phase could be determined as CrB. The main element in the dendrites is Ni, so that the dendrites are γ-Ni which is rich in Cr and Fe and poor in Nb.

Table 2 Compositional analysis of the structural constituents in the composite coating/wt%

Constituents	Ni	Cr	Fe	Si	Nb	C
White phases(including carbon)	2.46	1.46	1.20	0.41	64.88	29.59
White phases	3.34	2.04	1.65	0.61	92.35	
Dark whisker phases	3.99	86.09	4.56	0.81	4.55	
Dendrites	68.42	9.69	14.45	5.75	1.69	
Eutectics	72.01	5.93	11.99	5.42	4.65	
Eutectics (A region)	55.54	10.93	23.14	5.00	5.39	
Eutectics (B region)	73.06	4.94	11.18	6.95	3.87	

The interdendritic eutectic region, mainly containing Ni and a certain amount of Cr, Fe, Nb and Si, could not be identified in detail by SEM. Owing to the very fine microstructure, the SEM point compositional analysis could only represent average composition of the region. Fig. 4b shows high magnification SEM images of the interdendritic eutectics. It can be observed that the interdendritic eutectic displays feathered morphology, and is dispersed with dark fine precipitates in the white matrix. SEM EDS compositional analysis of the A (see A in Fig 4b) region and B (see B in Fig 4b) region in the eutectic structure are also shown in Table 2, with carbon and boron excluded. It indicates that the content of Cr and Fe in the A region are higher than B region, and the same as Ni in the B region. The formation of microstructure, during laser cladding of this group of Colmonoy series alloys, has been previously reported by several authors [11, 19-22]. Previously published works and the XRD results suggest that the interdendritic eutectic is, most certainly, consists of γ-Ni and $M_{23}C_6$ carbides. Finally, and according to the microstructure observed, the white phase can be identified as the γ-Ni phase and the dark fine precipitates as the $M_{23}C_6$. The analysis of the detailed microstructure of eutectic structure need to use other analytical techniques, such as transmission electron microscopy (TEM), it should be possible to find other interdendritic eutectics, as well as other compounds based on chromium carbides and

borides or even amorphous phases.

3.3 Formation mechanism of microstructure of composite coating

During laser cladding, The Ni-based alloy in the powder mixture is well melted and forms a molten pool due to its low melting temperature, and then Nb and C are melted directly or dissolved into the melt pool. In addition, niobium is a strong carbide-forming element and easy to be combined with carbon, and consequently niobium can react with carbon at such high temperature in the molten pool to form NbC.

NbC is well known to have high melting point (3600 ℃), so it precipitates from the alloy solution as the primary phase and freely grows up by absorbing the surrounding atoms of carbon and niobium. With the growth of NbC particles, the region surrounding them would be poor in carbon and niobium, while rich in chromium, boron and other solutes. This situation should be beneficial to the formation of CrB nuclei on the surface of NbC particles. In other words, the existing of NbC particles can provide the nucleation sites for CrB phases in the molten pool. Furthermore, with continuous cooling, CrB would be crystallized out from the alloy solution as another primary phase. CrB phases can be nucleated on NbC particles surface preferentially. EDS mapping analysis results of Nb, Cr and C at the region surrounding NbC particle are shown in Fig.5. The content of Nb and C in the white area are higher than other area, and the same as Cr in the dark area, which further confirm that the white phase is NbC particle and CrB phase can be nucleated on NbC particles surface preferentially.

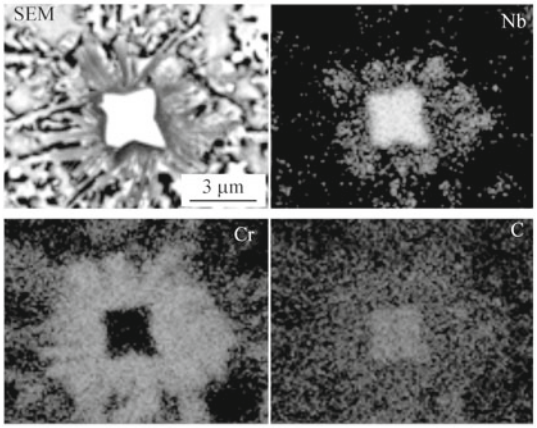

Fig.5 SEM images of surrounding NbC particle and EDS mapping analysis results of Nb, Cr, and C

With the decreasing temperature of molten pool, the remaining alloy solution is rapidly solidified as dual phase matrix. Since solidification is a fast and non-equilibrium process, the remaining alloy solution is not homogeneous in composition throughout the molten pool. The γ-Ni austenitic phase, a solid solution of Ni and Fe, would be formed where only Ni and Fe exist. The interdendritic eutectics of $M_{23}C_6$ with γ-Ni solid solution would be formed where not only the dominating Ni and Fe but also a small amount of Cr, Nb, and C exist. The formation of $M_{23}C_6$ instead of M_7C_3 could be due to the burning loss of graphite added or the combination of niobium and carbon during laser cladding which results in a lower content of C in the molten pool.

3.4 Microhardness of the coating

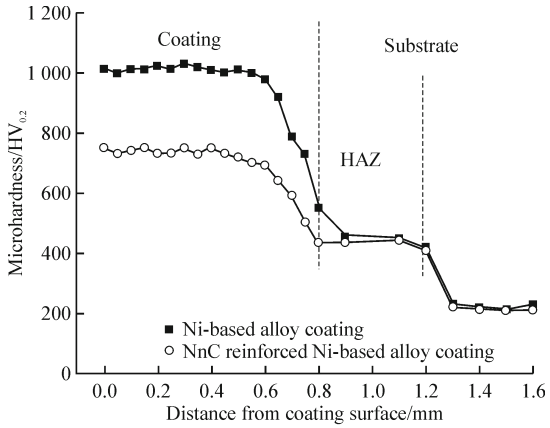

Fig.6 Microhardness distribution of coatings

The hardness profiles along the transverse section of the pure Ni-based alloy and NbC particles reinforced Ni-based alloy composite coating are shown in Fig.6. They similarly exhibit a stepwise characteristic and can be divided into three regions: coating, heat affected zone (HAZ) and substrate. The microhardness of the composite coating is markedly increased, giving a high average hardness of HV0.21000. Compared to the pure Ni-based alloy coating (HV0.2730), the microhardness of the composite coating is increased about 38%. This result can be attributed to the presence of lots of NbC particles with very high hardness formed in situ during laser cladding and as the primary reinforcements uniformly dispersed in the matrix. Moreover, the microhardness values only have slightly variety along the direction of thickness except for the bottom of coating, which is due in part to the uniform distribution of NbC particles in the coating because of the density of NbC nearing Ni-based alloy. With the increasing of the distance from the surface, the hardness decreases gradually and there is an abrupt decrease around the bonding interface. The reason is that the bottom of coating consists mainly of γ-Ni solid solution and its hardness is very lower. Owing to the occurrence of martensitic transformation, the hardness of the heat

affected zone (HAZ) of substrate near the interface is higher than the initial substrate.

3.5 Wear resistance of coatings

The wear loss of volume and wear rate as a function of sliding distance are shown in Fig.7, respectively. In the figures, the wear resistance of NbC particles reinforced Ni-based composite coating is compared with the pure Ni-based alloy coating at the same processing parameters. It can be seen that the in situ NbC reinforced Ni-based composite coating is more effective in improving wear resistance and has the smaller wear volume and also the lower wear rate with increasing sliding distance than the pure Ni-based alloy coating. Compared to the pure Ni-based alloy coating, the wear volume and wear rate of the composite coating are decreased about 39% and 32%, respectively. These experimental results show that the in situ synthesized NbC particles can effectively improve the wear resistance of the laser cladding Ni-based alloy coating.

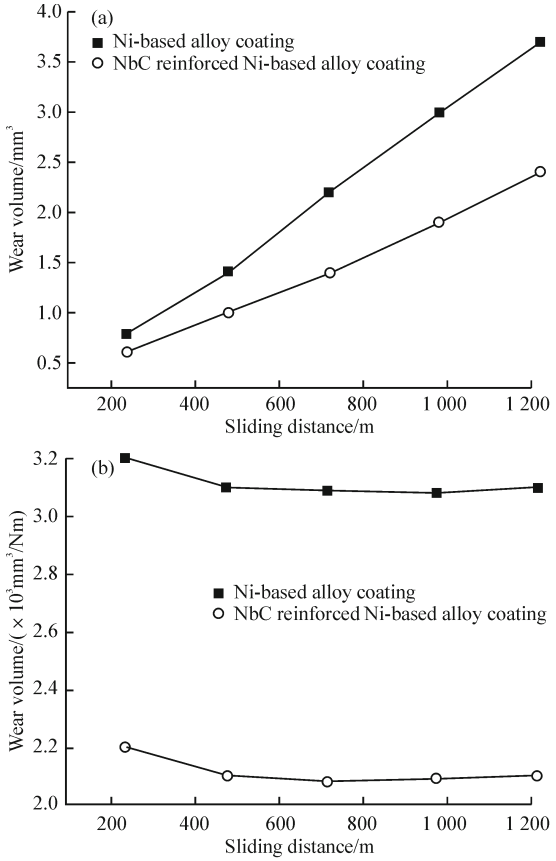

Fig.7 Changes in (a) wear loss of volume and (b) wear rate with sliding distance

The morphologies of worn surface for the NbC particles reinforced Ni-based composite coating and the pure Ni-based alloy coating are also shown in Fig.8, respectively. From the images we can know that the ploughed furrows and adhesive craters appear on

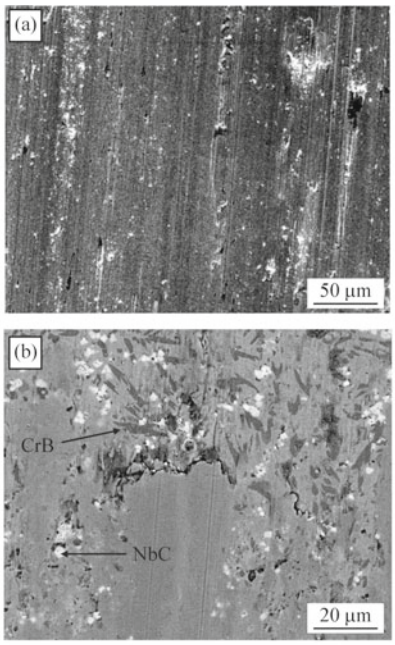

Fig.8 Worn surfaces of the coatings: (a) Ni-based alloy coating and (b) NbC particles reinforced Ni-based composite coating

the worn surface of the pure Ni-based alloy coating, demonstrating that the pure Ni-based alloy coating has the character of abrasive wear mechanism. In contrast to the pure Ni-based coating, the NbC particles reinforced Ni-based composite coating contains numerous fine in situ synthesized NbC particles which have higher strength than the $M_{23}C_6$ or M_7C_3 type carbides. They are tightly bound with the matrix and hardly to be fractured during wear tests. In addition, the composite coating has higher hardness comparing with the ring. Therefore, the worn surface of the NbC particles reinforced Ni-based composite coating is smooth and flat, on which only slight scratches exist, implying that the composite coating has very high resistance to wear.

4 Conclusions

A Ni-based alloy composite coating reinforced with NbC particles was successfully prepared on 1045 steel substrate by laser cladding. The NbC particles were introduced by in situ reacting niobium and graphite during laser cladding process, instead of NbC particles being added into molten pool directly. In situ synthesized NbC particles were distributed uniformly in the composite coating along the transverse section. An excellent metallurgical bond between the coating and the substrate was observed and the coating was free from cracks.

The microstructure of the coating was mainly

composed of NbC particles, CrB type chromium borides, γ-Ni primary dendrites and interdendritic eutectics, and the CrB phases often nucleated and grew on the surface of NbC particles or in their close vicinity. NbC particles were commonly precipitated in three kinds of morphologies, such as quadrangle, cluster and flower-like shape.

Compared with the pure nickel based alloy coating, the hardness and wear properties of the composite coating were significantly enhanced in virtue of the presence of in situ synthesized NbC particles and their well distribution in the coating.

References

[1] Sun R L, Lei Y W, Niu W. Laser Clad TiC Reinforced NiCrBSi Composite Coatings on Ti–6Al–4V Alloy Using a CW CO_2 Laser [J]. *Surf. Coat. Technol.,* 2009, 203 (10-11): 1 395-1 399

[2] Wang X H, Zhang M, Zou Z D, *et al.* Microstructure and Properties of Laser Clad TiC+NiCrBSi+Rare Earth Composite Coatings [J]. *Surf. Coat. Technol.,* 2002, 161 (2-3): 195-199

[3] Chen H H, Xu C Y, Chen J, *et al*. Microstructure and Phase Transformation of WC/Ni60B Laser Cladding Coatings during Dry Sliding Wear [J]. *Wear,* 2008, 264 (7-8): 487-493

[4] St-Georges L. Development and Characterization of Composite Ni–Cr + WC Laser Cladding [J]. *Wear,* 2007, 263 (1-6): 562-566

[5] Amado J M, Tobar M J, Alvarez J C. Laser Cladding of Tungsten Carbides (Spherotene®) Hhardfacing Alloys for the Mining and Mineral Industry [J]. *Appl. Surf. Sci.,* 2009, 255 (10): 5 553-5 556

[6] Herreraa Y, Grigorescu I C, Ramirez J, *et al*. Microstructural Characterization of Vanadium Ccarbide Laser Clad Coatings [J]. *Surf. Coat. Technol.,* 1998, 108–109 (1-3): 308-31

[7] Daniel B S S, Murthy V S R, Murty G S. Metal-ceramic Composites via in-situ Methods [J]. *J. Mater. Process. Technol.,* 1997, 68 (2): 132-155

[8] Matin M A, Lu L, Gupta M. Investigation of the Reactions between Boron and Titanium Compounds with Magnesium [J]. *Scr. Mater.,* 2001, 45 (4): 479-486

[9] Wang H Y, Jiang Q C, Li X L, *et al.* In situ Synthesis of TiC/Mg Composites in Molten Magnesium [J]. *Scr. Mater.,* 2003, 48 (9): 1 49-1 354

[10] Yang S, Liu W J, Zhong M L. In-situ TiC Reinforced Composite Coating Produced by Powder Feeding Laser Cladding [J]. *J. Mater. Sci. Technol.*, 2006, 22 (4): 519-525

[11] Wu X L. In situ Formation by Laser Cladding of a TiC Composite Coating with a Gradient Distribution [J]. *Surf. Coat. Technol.,* 1999, 115 (2-3): 111-115

[12] Yang S, Chen N, Liu W J, *et al.* Fabrication of Nickel Composite Coatings Reinforced with TiC Particles by Laser Cladding [J]. *Surf. Coat. Technol.,* 2004, 183 (2-3): 254-260

[13] Sun R L, Mao J F, Yang D Z. Microstructural Characterization of NiCr1BSiC Laser Clad Layer on Titaniumalloy Substrate [J]. *Surf. Coat. Technol.,* 2002, 150 (2-3): 199-204

[14] Zhong M L, Liu W J, Zhang Y, *et al.* Formation of WC/Ni Hard Alloy Coating by Laser Cladding of W/C/Ni Pure Element Powder Blend [J]. *Int. J. Refract. Met. Hard. Mater.,* 2006, 24 (6): 453-460

[15] Acchar W, Segadaes A M. Properties of Sintered Alumina Reinforced with Niobium Carbide [J]. *Int. J. Refract. Met. Hard. Mater.,* 2009, 27 (2): 427-430

[16] Huang S G, Liu R L, Li L, *et al*. NbC as Grain Growth Inhibitor and Carbide in WC–Co Hardmetals [J]. *Int. J. Refract. Met. Hard. Mater.,* 2008, 26 (5): 389-395

[17] Wang X H, Han F, Liu X M, *et al*. Effect of Molybdenum on the Microstructure and Wear Resistance of Fe-based Hardfacing Coatings [J]. *Mater. Sci. Eng., A,* 2008, 489 (1-2): 193-200

[18] zhang S H, Li M X, Cho T Y, *et al*. Laser Clad Ni-base Alloy Added Nano- and Micro-size CeO_2 Composites[J]. *Opt. Laser Technol.*, 2008, 40 (5): 716-722

[19] Li Q, Zhang D W, Lei T Q, *et al.* Comparison of Laser-clad and Furnace-melted Ni-based Alloy Microstructures[J]. *Surf. Coat. Technol.,* 2001, 137 (2-3): 122-135

[20] Navas C, Colaco R, Damborenea J de, *et al.* Abrasive Wear Behaviour of Laser Clad and Flame Sprayed-melted NiCrBSi Coatings [J]. *Surf. Coat. Technol.,* 2006, 200 (24): 6 854-6 862

[21] Zhang Da wei, Lei T C, Zhang J G, *et al.* The Effects of Heat Treatment on Microstructure and Erosion Properties of Laser Surface-clad Ni-base Alloy [J]. *Surf. Coat. Technol.,* 1999, 115 (2-3): 176-183

[22] Li Q, Lei T C, Chen W Z. Microstructural Characterization of Laser-clad TiCp-reinforced Ni–Cr–B–Si–C Composite Coatings on Steel [J]. *Surf. Coat. Technol.,* 1999, 114 (2-3): 278-284